Modeling, Simulation and Characterization of Atomic Force Microscopy Measurements for Ionic Transport and Impedance in PEM Fuel Cells:

GCEP Technical Report 2007

Investigators
Peter M. Pinsky, Professor, Mechanical Engineering; David M. Barnett, Professor, Materials Science and Engineering and Mechanical Engineering; Yongxing Shen, Graduate Research Assistant.

Abstract
The polymer electrolyte membrane fuel cell is a power source with the potential for reducing green-house gas emissions. Characterizing the electrolyte of a fuel cell is an important procedure for assessing the performance of the entire device. Atomic force microscopy (AFM) is one of the major instruments for such characterization, since it can be used for determining the surface potential and/or charge distributions in a fuel cell electrolyte. In order to understand the mechanisms involved in the AFM imaging of the membrane material, we have been developing detailed models that are able to describe the contributions from sample properties and AFM probe tip geometry to the AFM images.

In the past year, we have extended our initial model to take into account fuel cell electrolyte materials that are dielectric with spatial variation in charge distributions. This development allows us to accurately predict AFM images based on knowledge of the sample charge distribution and to characterize the resolution of the AFM. The proposed numerical method developed in this project also provides insights for the development of new algorithms for reconstructing sample charge distributions from AFM images, which would provide a comprehensive quantitative evaluation of fuel cell devices.

Introduction

Solid polymer fuel cells promise to be an efficient power source for mobile and stationary applications with the potential for a greatly reduced environmental impact. However, the ionic diffusion behavior under current load conditions in the ion-selective membranes of proton exchange membrane fuel cells (PEMFCs) is not completely understood. Further understanding of ion behavior at the Nernst diffusion layer of the membrane surface could enable development of new classes of solid polymer fuel cell membranes with increased mass transport.

In this project we are examining and characterizing the properties of solid polymer membranes through analytical and numerical modeling of ion transport, impedance,

diffusion and atomic force microscopy imaging. To address the challenges of enabling new solid polymer fuel cell membranes, the project has four primary objectives:

1. *Atomic force microscope imaging*. Nanoscale AFM surface imaging of dielectric or polarizable fuel cell materials involves complex AFM tip interactions with unknown surface and space charges resulting in electrostatic and van der Waals forces. Nonlinear modeling will be employed to solve the inverse problem of finding the charge distributions from AFM images with the goal of elucidating the mechanisms of charge motion in fuel cell and biological media relevant for environmental cleanup.

2. *Simulation of impedance measurements*. Modeling and simulation of AFM impedance measurements in fuel cells to shed light on the effects of probe tip geometry and surface roughness and topography with goal of developing scaling laws for fuel cell performance.

3. *Modeling of ionic transport in PEMFC's.* Analytical and numerical modeling of ionic diffusion in fuel cells taking into account electrochemical kinetics, current distribution, hydrodynamics and multi-component transport with the goal of elucidating mass transport characteristics.

4. *Particle diffusion modeling*. In order to further understand mechanisms of ion and solvent transport in hydrated PEMFC membranes, modeling that accounts for local molecular information will be employed.

Our primary efforts have been directed to the first objective.

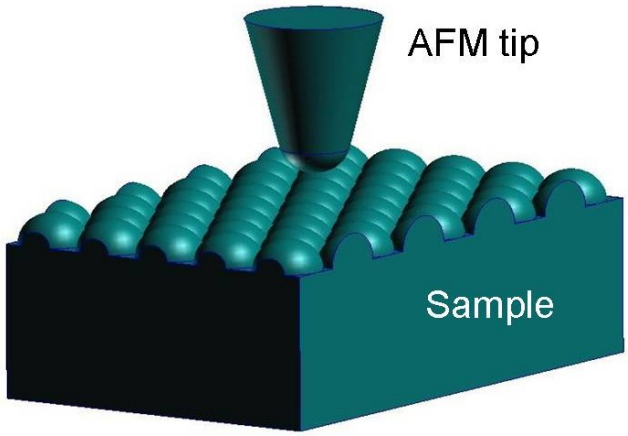

Figure 1: Schematic of the AFM tip (without the cantilever) and the sample

Background

Invented in 1986 [1], atomic force microscopy (AFM) has been and continues to be the prominent method for imaging and characterizing the surfaces of fuel cell electrolyte materials. Such imaging is absolutely essential for understanding why certain designs, selections, and processing of fuel cell membrane materials prove to be successful or unsuccessful choices. In this sense the AFM is currently as crucial to fuel cell technology development as is imaging by electromagnetic and other radiation in modern medicine and health care.

The key part of the atomic force microscope is a conical probe tip attached to the free end of a cantilever, as shown in Figure 1. As the probe scans a sample of interest, the AFM is able to produce images by recording the variation of some quantities related to the probe-sample interaction, e.g., the deflection or the oscillation amplitude of the cantilever. These images provide information about the fuel cell electrolyte, e.g. the surface topography and the charge distribution.

Of the existing experimental configurations of the AFM, electrostatic force microscopy (EFM) [2] and related techniques (e.g., Kelvin probe force microscopy (KPFM) [3] and scanning capacitance microscopy (SCM) [4]) use the Coulombic interaction between the AFM probe and the sample of interest as the source of information to generate images. These techniques can detect the existence and distribution of fuel cell charges. In order to separate the long-range electrostatic force from the short-range forces, such as van der Waals interaction and chemical bonding, the experiment requires a certain separation between the probe tip and the sample, ranging from 2 nm to 100 nm; hence, these techniques are categorized as *non-contact* atomic force microscopy.

A number of models describing probe-sample interactions have been proposed in the last two decades. Earlier models assumed the sample to be a semi-infinite conductor with a flat surface, which permitted the use of the image charge method. Within this framework, some models treated the probe surface as an equipotential with an assumed distribution of charges, such as a single point charge [6] or a uniformly charged line [7], and the probe-sample interaction was approximated as the interaction between the assumed charge distribution and its image with respect to the sample surface. Another group of models introduced geometric approximations to the probe shape and solved the probe-sample capacitance problem either by exactly solving the boundary value problem, e.g., the sphere model [8] and the hyperboloid model [9], or by introducing further approximations to the electric field between the probe and the sample [10—12]. These models provide convenient analytic expressions of the probe-sample interaction; however, more sophisticated models are demanded for studying the *lateral* variation of the sample surface properties (e.g., topography and trapped charge distribution) and the associated EFM measurements.

This demand has attracted researchers to attack the problem from different perspectives. Their models may be grouped into three families according to their

methodologies. One family of models invoked the molecular dynamics (MD) technique to track the motion of the atoms of the probe tip and the sample surface, while modeled the cantilever as a point mass to take into account its oscillation [13,14]. This model captured detailed atomic configurations of both solids and provided atomic-level information of the probe-sample interactions, including both Coulombic and van der Waals forces, and hence required reasonable initial conditions. And as for general MD systems, numerical artifacts were introduced to these models by the use of periodic boundary conditions.

A second family of models replaced the probe and the sample by a series of point charges and/or line charges and their image charges [15, 16]. Based on this method, interactions between the probe and a conductive or dielectric sample with topographic and/or dielectric in homogeneities [17—19] have been studied. This approach was capable of accommodating different scenarios, but the selection of source and test points may suffer from arbitrariness and might lack consistency between different selections.

The third family of approaches solved the well-defined electrostatic boundary value problem using continuum-level numerical schemes such as the finite element method [20], the self-consistent integral equation method [21], the multiple multipole program [22], and the boundary element method [23]. References [22] and [23] also provided de-convolution algorithms for conductive samples to reconstruct the tip-sample contact potential difference (CPD) from a KPFM measurement which the authors proved to be a convolution of the probe geometry and the CPD.

Of these models, the boundary element method proposed by Strassburg et al. [23] possesses advantages over other methods for modeling EFM in some important aspects. First, the EFM probe tip geometry can be exactly taken into account up to the discretization error, which permits comparison of different probe tip shapes. Second, no truncation is required for the vacuum domain (the space outside the probe and the sample) which has an infinite dimension but a uniform dielectric constant. Third, only surface discretization is required to solve the electrostatic problem; hence, there are fewer unknowns in the formulation than domain based techniques such as the finite element. For the case of a topographically flat sample, this reduction is even more pronounced, because the sample surface can be described using the image charge method and hence only the probe surface needs discretization.

Results

Boundary Element Modeling

In order to model the AFM measurements on fuel cell electrolyte materials which are usually dielectrics (e.g., yttria stabilized zirconia and gadolinia doped ceria[1]), we

[1] We are using *solid oxide* fuel cell electrolyte materials as our model materials since their charge distributions are better known compared to *polymer electrolytes.* However, our formulation and numerical scheme also apply to polymer electrolytes.

have generalized the formulation of Strassburg et al. [23] to the case of a dielectric sample.

For the system with the AFM and a dielectric sample, the governing partial differential equations are

$$\nabla^2\phi = 0 \quad \text{in vacuum;} \tag{1}$$

$$\nabla^2\phi = -\rho/\kappa\varepsilon_0 \quad \text{in the sample,} \tag{2}$$

where ϕ denotes the electrostatic potential, ∇^2 is the Laplacian operator, ρ the local volumetric charge density of the sample, κ the sample dielectric constant (assumed isotropic and homogenous), and $\varepsilon_0 = 8.8542\times10^{-12}$ F/m is the vacuum permittivity.

The boundary condition on the probe tip surface is given by the bias V applied between the probe and the sample. We arbitrarily assume the back side (the side opposite to the probe) of the sample is grounded, and the potential on the probe is denoted by V, i.e.

$$\phi = V \quad \text{on} \quad S_t \quad \text{(probe tip surface).} \tag{3}$$

The continuity condition across the sample surface can be obtained via the Gauss flux theorem to find

$$\phi|_{\mathrm{v}} = \phi|_{\mathrm{s}}, \qquad \left.\frac{\partial\phi}{\partial\mathbf{n}}\right|_{\mathrm{v}} = \kappa\left.\frac{\partial\phi}{\partial\mathbf{n}}\right|_{\mathrm{s}} - \sigma_{\mathrm{s}}, \tag{4}$$

where subscripts v and s denote whether the value is evaluated on the vacuum side or sample side, respectively. $\mathbf{n}$ is the outward surface normal of the sample. σ_{s} is the trapped surface charge density of the sample.

Equations (1)—(4) uniquely determine the entire electric field. To solve for this field, we apply Green's second identity to obtain the equivalent boundary integral equation for the case in which the sample has a flat surface:

$$\begin{aligned}&\int_{S_t}\left[G(\mathbf{r};\mathbf{r}') - \frac{\kappa-1}{\kappa+1}G(\mathbf{r};\bar{\mathbf{r}}')\right]\sigma(\mathbf{r})\mathrm{d}S(\mathbf{r}) = \\ &V - \frac{2}{\kappa+1}\int_{S_s}G(\mathbf{r};\mathbf{r}')\sigma_{\mathrm{s}}(\mathbf{r})\mathrm{d}S(\mathbf{r}) - \frac{2}{\kappa+1}\int_{\Omega_s}G(\mathbf{r};\mathbf{r}')\rho(\mathbf{r})\mathrm{d}\Omega(\mathbf{r}), \forall\mathbf{r}'\in S_t\end{aligned} \tag{5}$$

where S_s and Ω_s denote the sample surface and volumetric domain, respectively, $G(\mathbf{r};\mathbf{r}') \equiv (4\pi\varepsilon_0 |\mathbf{r}-\mathbf{r}'|)^{-1}$ is the infinite medium Green's function for electrostatics, σ is the unknown charge density of the probe tip surface, and $\bar{\mathbf{r}}'$ is the mirror image position of $\mathbf{r}'$ with respect to the sample surface.

The boundary integral equation (5) can be solved using standard boundary element method. Upon solving (5), the probe-sample interaction can be obtained via the Maxwell stress tensor as

$$\mathbf{f} = \frac{1}{2\varepsilon_0}\int_{S_t} \sigma^2 \mathbf{n} dS ,$$

where $\mathbf{n}$ is the outward surface normal of the probe tip.

Case studies

With the methodology described above, we have studied two special cases of sample charge distributions to predict their AFM images.

Case 1: Sample with point charges on the surface

We consider a sample with two positive point charges on its surface, each of which has a magnitude of one elementary charge (e = 1.6099×10^{-19}C). With the boundary element method, we have predicted the AFM probe-sample interaction as the probe scans the sample with constant separation. We have plotted this force as a function of the tip horizontal position in Figure 2 for different spacings of these two charges, i.e., 0, $R/2$, R, and $2R$, where R denotes the tip apex radius. Here zero spacing is the case in which the two point charges coincide with each other, i.e., a single charge with a magnitude of $2e$.

The curves in Figure 2 illustrate the convolution effect between a finite tip and infinitesimal sample features. In this particular case, the probe's capability of distinguishing contributions from different sources to the overall probe-sample interaction is limited by the probe tip apex curvature.

Case 2: Sample with grain boundaries having segregated charges

As was previously reported by Aoki et al.[24], grain boundary segregation is a common phenomenon in some doped ionic crystals such as yttria-stabilized-zirconia (YSZ) Due to such segregation, excess charges are present adjacent to the grain

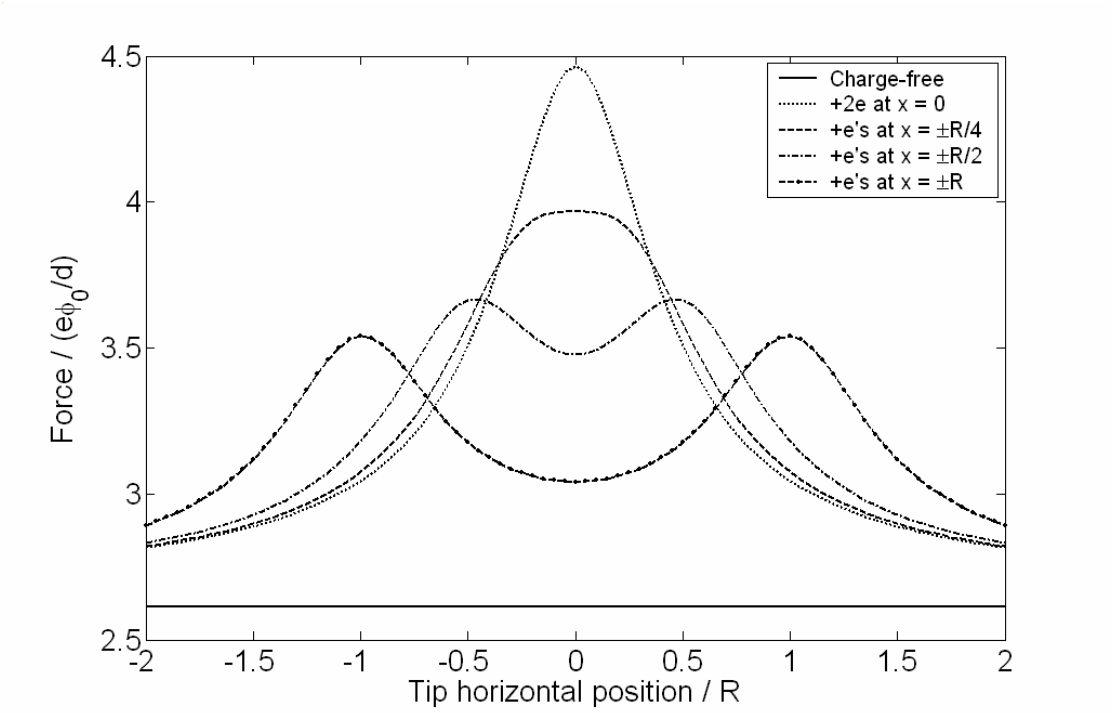

Figure 2 Probe-sample forces vs tip horizontal position for unit bias applied between a probe and dielectric samples with point charge(s) located at the surface. The dotted (..) curve is for a positive point charge of magnitude 2*e* located at $x = 0$, where $e = 1.6099\times10^{-19}$C is the elementary charge. The dashed (- -) curve, the dash-dotted (-.-.) curve, and the dash-dash-dotted (- -.- -.) curve are for two positive point charges with magnitudes e located at x = ±5, 10, and 20 nm, respectively. The solid curve is for a charge-free sample as a reference. The sample is assumed to be semi-infinite with a flat surface. The probe is conical with a spherical apex and a radius of curvature 20 nm. The total height of the probe is 15 μm. The semi-angle of the cone is 15°. The bias applied between the probe and the sample back side is 1 V. The dielectric constant of the sample κ is taken to be 40.0. The probe-sample separation *d* is 2 nm.

boundaries. We propose a model to describe such grain boundaries as sheets of charges inside the sample as illustrated in Figure 3. With this treatment, the AFM measurements on such samples can be predicted and we plot them in Figure 4. Similar conclusions can be drawn as in Case 1.

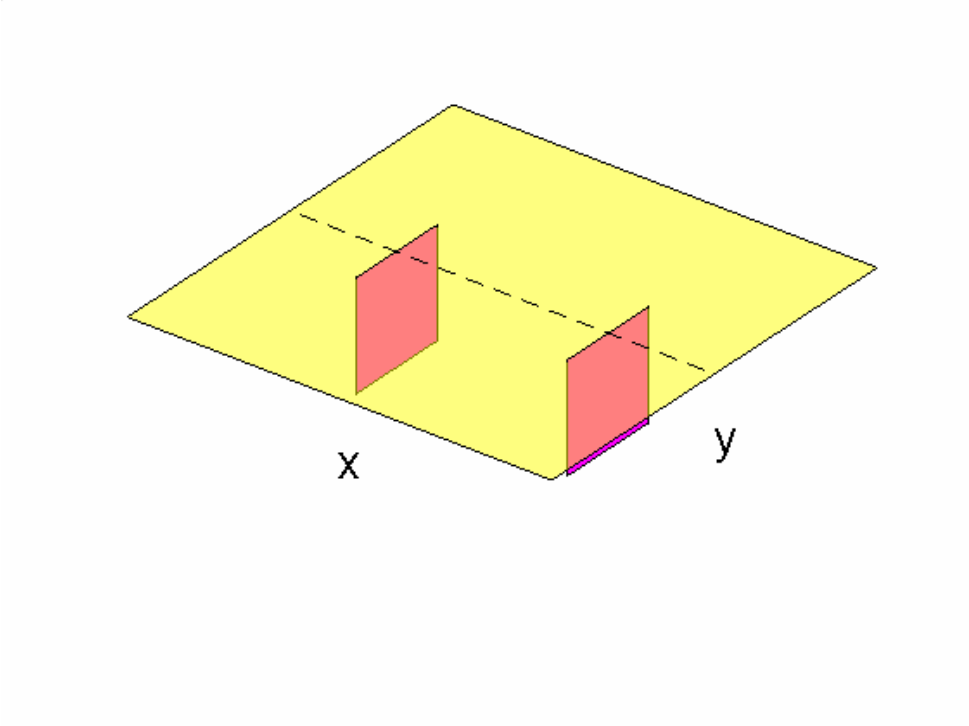

Figure 3 Schematic of a sample with two rectangular-shaped grain boundaries located parallel to the *y*, *z*-plane. The dashed line illustrates the trajectories of the AFM tip *projected* on the sample surface.

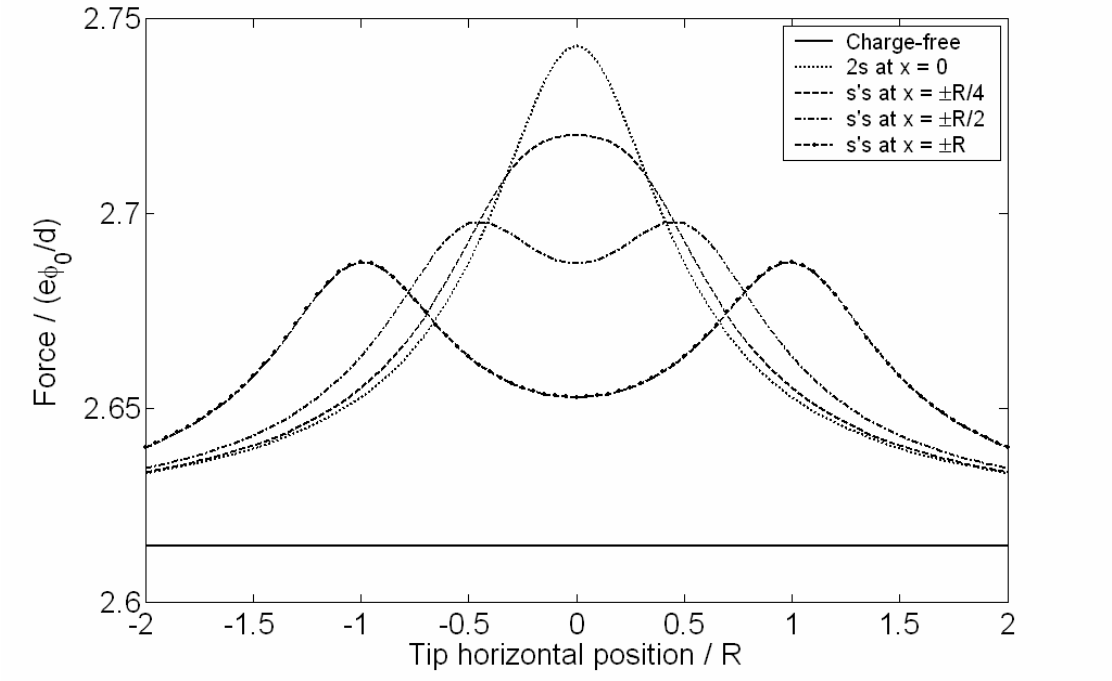

Figure 4 Probe-sample forces vs tip horizontal position for unit bias applied between a probe and dielectric samples with square grain boundary(ies) with dimensions $a \times a$ located near the surface, where $a = 0.5139$ nm is the lattice constant of yttria-stabilized-zirconia (YSZ).

These grain boundaries parallel the *y, z*-plane. The dotted (..) curve is for a single grain boundary of charge density 2*s* located at $x = 0$, where $s = +e/a^2$. The dashed (- -) curve, the dash-dotted (-.-.) curve, and the dash-dash-dotted (- -.- -.) curve are for two grain boundaries with charge densities *s* located at $x = \pm 5$, 10, and 20 nm, respectively. The solid curve is for a charge-free sample as a reference. The parameters of the probe and the sample are the same as those used in Figure 2.

Progress

We have developed a numerical scheme that is able to predict the electrostatic interaction between an AFM and a dielectric sample such as fuel cell electrolyte. AFM images can be seen as convolutions of the sample charge density and the probe tip geometry. De-convolution algorithms for isolating desired information from artifacts can be constructed based on the solution to the forward problem, providing a way to determine localized information about the fuel cell electrolyte and to help assess the quality of the fuel cell.

Future Plans

1. Developing de-convolution methods to determine fuel cell charge distributions from AFM measurements as a solution to the inverse problem
2. Modeling the impedance measurements involved in fuel cell characterization
3. Modeling ion transports through PEM fuel cells

Publications

1. Y. Shen, D. M. Barnett and P. M. Pinsky, Integral equation modeling of electrostatic interactions in atomic force microscopy, in C. Constanda (Ed.): Integral Methods in Science and Engineering 9, 2007 (in press).
2. Y. Shen, D. M. Barnett and P. M. Pinsky, Modeling electrostatic force microscopy for conductive and dielectric samples using the boundary element method, in preparation.
3. Y. Shen, M. Lee, W. Lee, D. M. Barnett, P. M. Pinsky and F. B. Prinz, Resolution and image broadening study for electrostatic force microscopy using the boundary element method, in preparation.

References

1. Binnig, G., Quate, C.F., and Gerber, Ch., Atomic force microscope, Phys. Rev. Lett., 56, 930-933, 1986.
2. Stern, J.E., Terris, B.D., Mamin, H.J., and Rugar, D., Deposition and imaging of localized charge on insulator surfaces using a force microscope, Appl. Phys. Lett., 53, 2717-2719, 1988.
3. Nonnenmacher, M., O'Boyle, M.P., and Wickramasinghe, H.K., Kelvin probe force microscopy, Appl. Phys. Lett., 58, 2921–2923, 1991.

4. Williams, C.C., Hough, W.P., and Rishton, S.A., Scanning capacitance microscopy on a 25 nm scale, Appl. Phys. Lett., 55, 203-205, 1989.
5. Girard P., Electrostatic force microscopy: principles and some applications to semiconductors, Nanotechnology, 12, 485-490, 2001.
6. Hu, J., Xiao, X.-D., Ogletree, D.F., and Salmerón, M., Imaging the condensation and evaporation of molecularly thin films of water with nanometer resolution, Science, 268, 267-269, 1995.
7. Hao, H.W., Baró, A.M., and Sáenz, J.J., Electrostatic and contact forces in force microscopy, J. Vac. Sci. Technol. B, 9(2), 1323-1328, 1991.
8. Terris, B.D., Stern, J.E., Rugar, D., and Mamin, H.J., Contact electrification using force microscopy, Phys. Rev. Lett., 63 (24), 2669-2672, 1989.
9. Pan, L.H., Sullivan, T.E., Peridier, V.J., Cutler, P.H., and Miskovsky, N.M., Three-dimensional electrostatic potential, and potential-energy barrier, near a tip-base junction, Appl. Phys. Lett., 65, 2151-2153, 1994.
10. Hochwitz, T., Henning, A.K., Levey, C., Daghlian, C., and Slinkman, J., Capacitive effects on quantitative dopant profiling with scanned electrostatic force microscopes, J. Vac. Sci. Technol. B, 14, 457–462, 1996.
11. Hudlet, S., Saint Jean, M., Guthmann, C., and Berger, J., Evaluation of the capacitive force between an atomic force microscopy tip and a metallic surface, Eur. Phys. J. B, 2, 5-10, 1998.
12. Colchero, J., Gil, A., and Baró, A. M., Resolution enhancement and improved data interpretation in electrostatic force microscopy, Phys. Rev. B, 64, 245403, 2001.
13. Livshits, A.I., Shluger, A.L., Rohl, A.L., and Foster, A.S., Model of noncontact scanning force microscopy on ionic surfaces, Phys. Rev. B, 59, 2436-2448, 1999.
14. Barth, C., Foster, A.S., Reichling, M., and Shluger, A.L., Contrast formation in atomic resolution scanning force microscopy on CaF_2(111): experiment and theory, J. Phys.: Condens. Matter, 13, 2061-2079, 2001.
15. Mesa, G., Dobado-Fuentes, E., and Sáenz, J.J., Image charge method for electrostatic calculations in field-emission diodes, J. Appl. Phys., 79, 39-44, 1996.
16. Belaidi, S., Girard, P., and Leveque, G., Electrostatic forces acting on the tip in atomic force microscopy: Modelization and comparison with analytic expressions, J. Appl. Phys., 81 (3), 1023-1030, 1997.
17. Gómez-Moñivas, S., and Sáenz, J.J., Theory of electrostatic probe microscopy: A simple perturbative approach, Appl. Phys. Lett., 76, 2955-2957, 2000.
18. Gómez-Moñivas, S., Froufe-Pérez, L., Caamaño, A.J., and Sáenz, J.J., Electrostatic force between sharp tips and metallic and dielectric samples, Appl. Phys. Lett., 79, 4048-4050, 2001.
19. Sacha G.M., Gómez-Navarro, C., Sáenz, J.J., and Gómez-Herrero, J., Quantitative theory for the imaging of conducting objects in electrostatic force microscopy, Appl. Phys. Lett., 89, 173122, 2006.
20. Belaidi, S., Lebon, E., Girard, P., Leveque, G., and Pagano, S., Finite element simulations of the resolution in electrostatic force microscopy, Appl. Phys. A, 66, S239-S243, 1998.

21. Li, Z.-Y., Gu, B.-Y., and Yang, G.-Z., Scanning-electrostatic-force microscopy: Self-consistent method for mesoscopic surface structures, Phys. Rev. B, 57, 9225–9233, 1998.
22. Jacobs, H.O., Leuchtmann, P., Homan, O.J., and Stemmer, A., Resolution and contrast in Kelvin probe force microscopy, J. Appl. Phys., 84, 1168–1173, 1998.
23. Strassburg, E., Boag, A., and Rosenwaks, Y., Reconstruction of electrostatic force microscopy images, Rev. Sci. Instrum., 76, 083705, 2005.
24. Aoki, M., Chiang, Y.M., Kosacki, I., Lee, I.J.R., Tuller, H., and Liu, Y.P., Solute segregation and grain-boundary impedance in high-purity stabilized zirconia, J. Am. Ceram. Soc., 79, 1169-1180, 1996.

Contacts

Peter M. Pinsky: pinsky@stanford.edu
David M. Barnett: barnett@stanford.edu